

## Growth of Alumina Overlayer Deposited on Au<sub>101</sub>/TiO<sub>2</sub> Catalyst Model Via Atomic Layer Deposition

Mohammed Z. Asiri<sup>1-3</sup>, Arthaya Kai<sup>1</sup>, Heike Ebendorff-Heidepriem<sup>4</sup>, Rohul H. Adnan,<sup>5</sup> Thomas D. Small<sup>2</sup>, Thomas Ceme<sup>3</sup>, Gregory F Metha<sup>2</sup>, Gunther G. Andersson<sup>1</sup>.

<sup>1</sup>*Flinders Institute for Nanoscale Science and Technology and Flinders Microscopy and Microanalysis, College of Science and Engineering, Flinders University, Adelaide, South Australia 5042, Australia.*

<sup>2</sup>*Department of Chemistry, University of Adelaide, Adelaide, South Australia 5005, Australia.*

<sup>3</sup>*Department of Physics, College of Science and Humanities in Al-Kharj, Prince Sattam Bin Abdulaziz University, Al-Kharj 11942, Saudi Arabia*

<sup>4</sup>*Institute for Photonics and Advanced Sensing (IPAS) and the School of Physics, Chemistry and Earth Sciences, The University of Adelaide, Adelaide 5000, Australia.*

<sup>5</sup>*Physical Science and Engineering Division, King Abdullah University of Science and Technology (KAUST), Thuwal 23955-6900, Saudi Arabia*

### Contents

List of samples .....	4
ARXPS Section.....	4
A single ALD Cycle results (ARXPS) .....	6
5 ALD Cycle results (ARXPS).....	9
10 ALD Cycle results (ARXPS).....	10
XPS Section .....	12
ISS Section.....	13
ISS Monolayer Calculations .....	15
NICISS Section.....	17
Determining the position of O of AlO <sub>x</sub> in XPS .....	17
Iodine Exposure Experiment .....	18
References.....	20

### List of Figures

Figure S1: High-resolution XP spectra of 1 ALD-AlO <sub>x</sub> deposited onto RF-sputtered TiO <sub>2</sub> , fitted with a Shirley background, representing the respective elements of (A) C 1s, (B) O 1s, (C) Ti 2p, (D) Al 2p measured at a 0° emission angle. ....	7
Figure S2: High-resolution XP spectra of 1 ALD-AlO <sub>x</sub> deposited onto RF-sputtered TiO <sub>2</sub> , fitted with a Shirley background, representing the respective elements of (A) C 1s, (B) O 1s, (C) Ti 2p, (D) Al 2p measured at a 60° emission angle. ....	8

Figure S3: Variation in the ARXPS intensity of measured elements C, O, Ti, and Al versus the emission angles, solid lines connect the fitted intensity ratios, and the dashed lines connect the relative intensity of the measured data for the sample with deposition.....	8
Figure S4: The concentration depth profile of the 1 ALD Cycle sample. The model presents the atomic densities of each emitting constituent element versus the depth in Angstrom (Å) within each respective layer. ....	9
Figure S5: High-resolution XP spectra of 5 ALD-AlO <sub>x</sub> deposited onto RF-sputtered TiO <sub>2</sub> , fitted with a Shirley background, representing the respective elements of (A) C 1s, (B) O 1s, (C) Ti 2p, (D) Al 2p measured at a 60° emission angle. ....	10
Figure S6: High-resolution XP spectra of 10 ALD-AlO <sub>x</sub> deposited onto RF-sputtered TiO <sub>2</sub> , fitted with a Shirley background, representing the respective elements of (A) C 1s, (B) O 1s, (C) Ti 2p, (D) Al 2p measured at a 0° emission angle. ....	11
Figure S7: High-resolution XP spectra of 10 ALD-AlO <sub>x</sub> deposited onto RF-sputtered TiO <sub>2</sub> , fitted with a Shirley background, representing the respective elements of (A) C 1s, (B) O 1s, (C) Ti 2p, (D) Al 2p measured at a 60° emission angle. ....	12
Figure S8: Variation in the ARXPS intensity of measured elements C, O, Ti, and Al versus the emission angles, solid lines connect the fitted intensity ratios, and the dashed lines connect the relative intensity of the measured data for the sample with deposition.....	13
Figure S9: The concentration depth profile of the 10 ALD Cycles sample. The model presents the atomic densities of each emitting constituent element versus the depth in Angstrom (Å) within each respective layer. ....	13
Figure S10: The high-resolution spectra of P 2p of the phosphine ligands (A) before ALD, and (B) after ALD of 1, 5, and 10 ALD cycles.....	14
Figure S11: ISS survey spectra for Au <sub>101</sub> /TiO <sub>2</sub> sample. In the legend the number of sputtered monolayers is shown. ....	15
Figure S12: ISS survey spectra for 5 ALD AlO <sub>x</sub> /Au <sub>101</sub> /TiO <sub>2</sub> sample. ....	16
Figure S13: (A) NICIS spectra of gold and gold coated with 2 and 5 cycles of ALD-AlO <sub>x</sub> (B) NICIS spectra of titanium without ALD, with 2 and 5 cycles of ALD-AlO <sub>x</sub> .....	18
Figure S14: (A) O 1s spectrum for the O fitted with doublet peaks before heating the sample. (B) After heating the O 1s spectrum for the O fitted with a single peak. ....	18
Figure S15: Absorption spectra of the iodine-iodide solution before and after exposure to Au <sub>101</sub> /TiO <sub>2</sub> with Al <sub>2</sub> O <sub>3</sub> overlayer samples for 10 h. Measurements performed with a Cary 3500 UV-Vis spectrophotometer. ....	19

Figure S16: (A) Au 4f spectrum of the sample 5 ALD on Au<sub>101</sub>/TiO<sub>2</sub> before iodine exposure. (B) Al 2p spectrum before iodine exposure of the sample 5 ALD on Au<sub>101</sub>/TiO<sub>2</sub>. (C) Au 4f spectrum after iodine exposure, and (D) Al 2p spectrum after iodine exposure.....20

Figure S17: UV-vis absorption spectrum of Au<sub>101</sub> in dichloromethane. ....21

**List of Tables**

Table S1: List of samples investigated through this project. ....3

Table S2: Elemental composition of each species of the samples of 1 ALD, 5 ALD, and 10 ALD for 0°, 30°, 45°, 55°, and 60° angles of observations. ....4

Table S3: XPS calibrated peaks positions(eV) of 1 ALD, 5 ALD, and 10 ALD samples for 0°, 30°, 45°, 55°, and 60° angles of observations. ....5

Table S4: Peak positions, peak intensity, and elemental composition of sample 1, 5, and 10ALD cycles of Au<sub>101</sub>/TiO<sub>2</sub> sample. ....11

Table S5: Fraction of Al and Au remaining on the TiO<sub>2</sub> surface after applying the iodine procedure. For the calculation only the XPS peaks for the elements forming the substrate have been used, i.e. the O peak at 530.5 eV, the Ti, Al and Au peaks. The other O peaks and C are changing as well but only reflect the surface contamination due to the application of the iodine procedure and are thus not relevant for the analysis. ....19

## List of samples

Table S1: List of samples investigated through this project.

Samples	Composition	Characterisation
<b>Free of Au<sub>101</sub> Samples</b>		
0 ALD	TiO <sub>2</sub>	XPS, and ARXPS
1 ALD	AlO <sub>x</sub> /TiO <sub>2</sub>	XPS, and ARXPS
5 ALD	AlO <sub>x</sub> /TiO <sub>2</sub>	XPS, and ARXPS
10 ALD	AlO <sub>x</sub> /TiO <sub>2</sub>	XPS, and ARXPS
<b>Samples with Au<sub>101</sub> clusters</b>		
0 ALD	Au <sub>101</sub> /TiO <sub>2</sub>	XPS, ISS, and NICISS
1 ALD	AlO <sub>x</sub> /Au <sub>101</sub> /TiO <sub>2</sub>	XPS
2 ALD	AlO <sub>x</sub> /Au <sub>101</sub> /TiO <sub>2</sub>	NICISS
5 ALD	AlO <sub>x</sub> /Au <sub>101</sub> /TiO <sub>2</sub>	XPS, ISS, and NICISS
10 ALD	AlO <sub>x</sub> /Au <sub>101</sub> /TiO <sub>2</sub>	XPS
<b>Investigation samples</b>		
Calibration Sample	Au/TiO <sub>2</sub>	XPS
Al foil sample	Al foil	XPS
O identification sample	Au/SiO <sub>2</sub>	XPS

## ARXPS Section

The ARXPS concentration depth profile are determined by fitting the measured intensity ratios of each elemental species with calculated intensity ratios through an ARXPS model. In the model the sample is divided into layers with homogeneous thickness and the intensity of electrons emitted of each elemental species forming a given layer is calculated using:

$$I(i,j, \theta) = \frac{d\sigma_i}{d\Omega} n_i(j) \lambda_j(\theta) \left[ 1 - \exp\left(-\frac{d_j}{\lambda_j(\theta)}\right) \right] \prod_{m=1}^{j-1} \exp\left(-\frac{d_m}{\lambda_m(\theta)}\right) \quad eq. 1$$

where:

$n_i$  is the number density of elemental species  $i$ , and  $z$  the depth.

$E$  the kinetic energy.

$d\sigma/d\Omega$  the differential photoionization cross-section of the core level of the respective element.

$\lambda$  the electron attenuation length (EAL).

From eq. 1 the relative intensity of each elemental species is calculated. The fitting procedure is based on the following principles:

1. The sample is modelled as a series of finite layers, each with a homogeneous composition and homogeneous thickness. The effective attenuation length (EAL) of electrons varies depending on the composition of each layer.
2. The thickness and composition of each layer are the fitting parameters.
3. The inelastic mean free path (IMFP) of electrons is dependent on their kinetic energy and are taken from<sup>1</sup>.
4. The photoionization cross sections of the elements are taken from<sup>2</sup>.
5. The thickness of the TiO<sub>2</sub> substrate is assumed to be infinite.
6. Atomic densities (atoms/Å<sup>3</sup>) are used to represent the relative depth profile of each element within a layer.

From the concentration depth profiles, the thickness of the ALD layers can be estimated. The layer composition is expressed in terms of atomic densities (atoms/Å<sup>3</sup>) as illustrated in<sup>3</sup>.

*Table S2: Elemental composition of each species of the samples of 1 ALD, 5 ALD, and 10 ALD for 0°, 30°, 45°, 55°, and 60° angles of observations.*

ALD Cycles	Emission Angles (θ)	C 1	C 2	C 3	O 1	O 2	Ti	Al
1 ALD	0°	14.2	1.5	0.5	56.5	3.8	20.9	2.5
	30°	15.3	2.4	0.8	55.0	4.1	20.0	2.5
	45°	19.1	2.9	0.8	52.4	4.4	17.8	2.5
	55°	22.2	3.1	0.6	50.4	4.6	16.7	2.4
	60°	22.0	3.8	1.0	49.3	5.8	16.2	2.7
5 ALD	0°	16.1	1.7	0.6	54.0	4.6	19.8	3.3
	30°	17.9	1.8	0.5	52.3	4.6	18.7	4.2
	45°	19.4	2.3	0.6	50.8	5.0	18.1	3.8
	55°	21.9	3.1	1.1	48.8	4.8	16.2	4.1
	60°	23.9	3.5	1.0	47.3	4.9	15.3	4.1
10 ALD	0°	18.0	2.5	0.7	49.3	7.6	15.6	6.4
	30°	20.4	3.1	1.1	47.5	7.7	13.9	6.2
	45°	23.0	4.6	1.4	44.5	7.9	12.2	6.5
	55°	25.2	5.4	1.6	42.0	7.8	11.0	6.9
	60°	25.8	5.57	1.3	42.2	8.2	10.2	6.7

Table S3: XPS calibrated peaks positions(eV) of 1 ALD, 5 ALD, and 10 ALD samples for 0°, 30°, 45°, 55°, and 60° angles of observations.

ALD Cycles	Emission Angle (θ)	C 1 Position (eV)	C 2 Position (eV)	C 3 Position (eV)	O 1 Position (eV)	O 2 Position (eV)	Ti Position (eV)	Al Position (eV)
1 ALD	0°	284.4	286.0	287.7	530.5	532.0	459.2	74.5
	30°	284.4	285.7	287.4	530.5	532.0	459.2	74.5
	45°	284.4	286.0	287.7	530.5	532.1	459.2	74.4
	55°	284.4	286.1	288.1	530.5	532.1	459.2	74.4
	60°	284.4	285.8	287.3	530.5	532.2	459.2	74.4
5 ALD	0°	284.3	285.7	287.4	530.5	531.9	459.2	74.6
	30°	284.3	285.9	287.9	530.5	531.9	459.2	74.6
	45°	284.4	285.8	287.5	530.5	532.0	459.2	74.6
	55°	284.4	285.7	287.1	530.5	532.1	459.2	74.6
	60°	284.4	285.9	287.9	530.5	532.1	459.2	74.6
10 ALD	0°	284.3	285.7	287.3	530.5	532.0	459.2	74.6
	30°	284.3	285.9	287.5	530.5	532.0	459.2	74.6
	45°	284.3	285.7	287.4	530.5	532.1	459.2	74.6
	55°	284.4	285.8	287.5	530.6	532.2	459.2	74.6
	60°	284.4	285.7	287.4	530.6	532.3	459.2	74.6

#### A single ALD Cycle results (ARXPS)

The XP spectra of C 1s, O 1s, Ti 2p, and Al 2p for the sample of 1 ALD cycle deposited on plane TiO<sub>2</sub> surface. The spectra show in Figure S1, and S2 for 0° of observation and 60°, respectively.

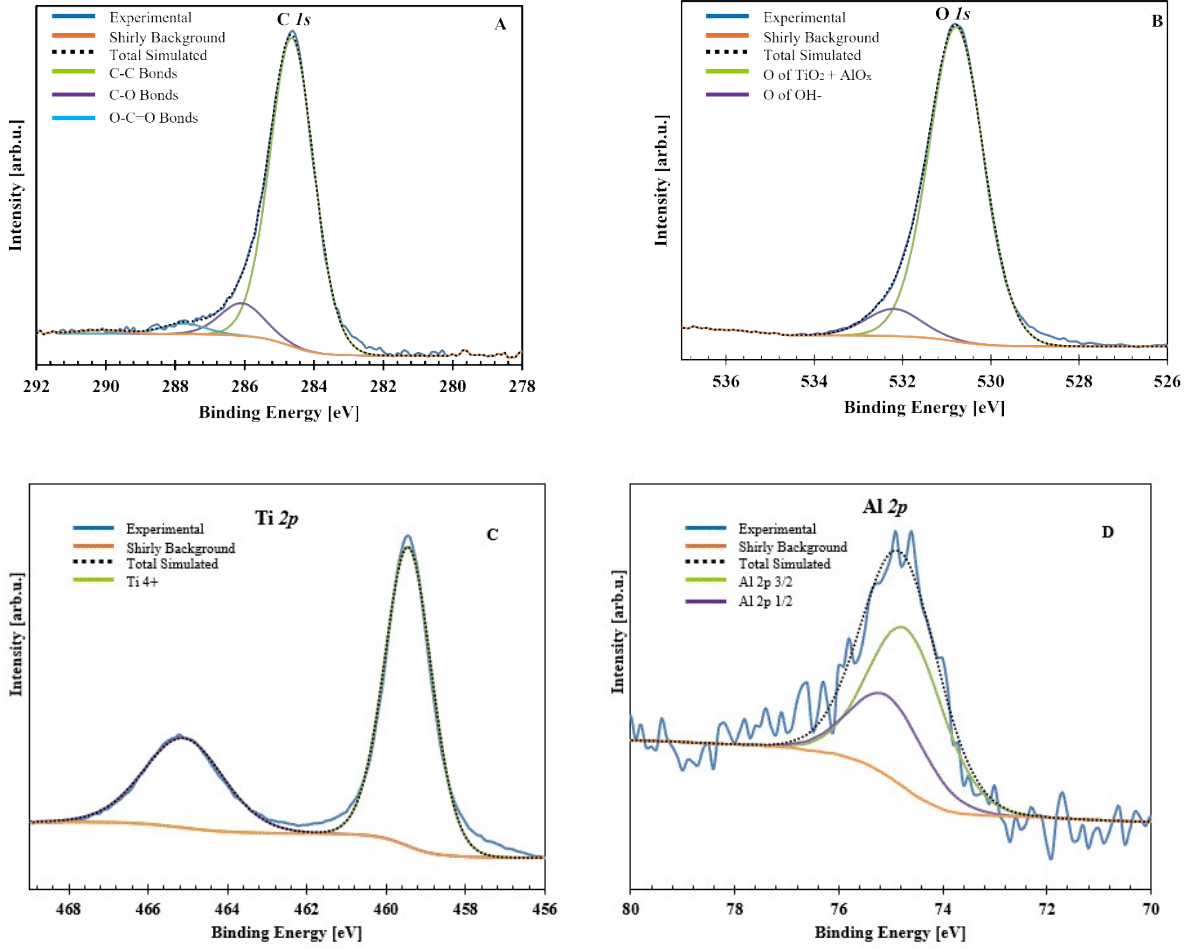


Figure S1: High-resolution XPS spectra of 1 ALD- $\text{AlO}_x$  deposited onto RF-sputtered  $\text{TiO}_2$ , fitted with a Shirley background, representing the respective elements of (A) C 1s, (B) O 1s, (C) Ti 2p, (D) Al 2p measured at a  $0^\circ$  emission angle.

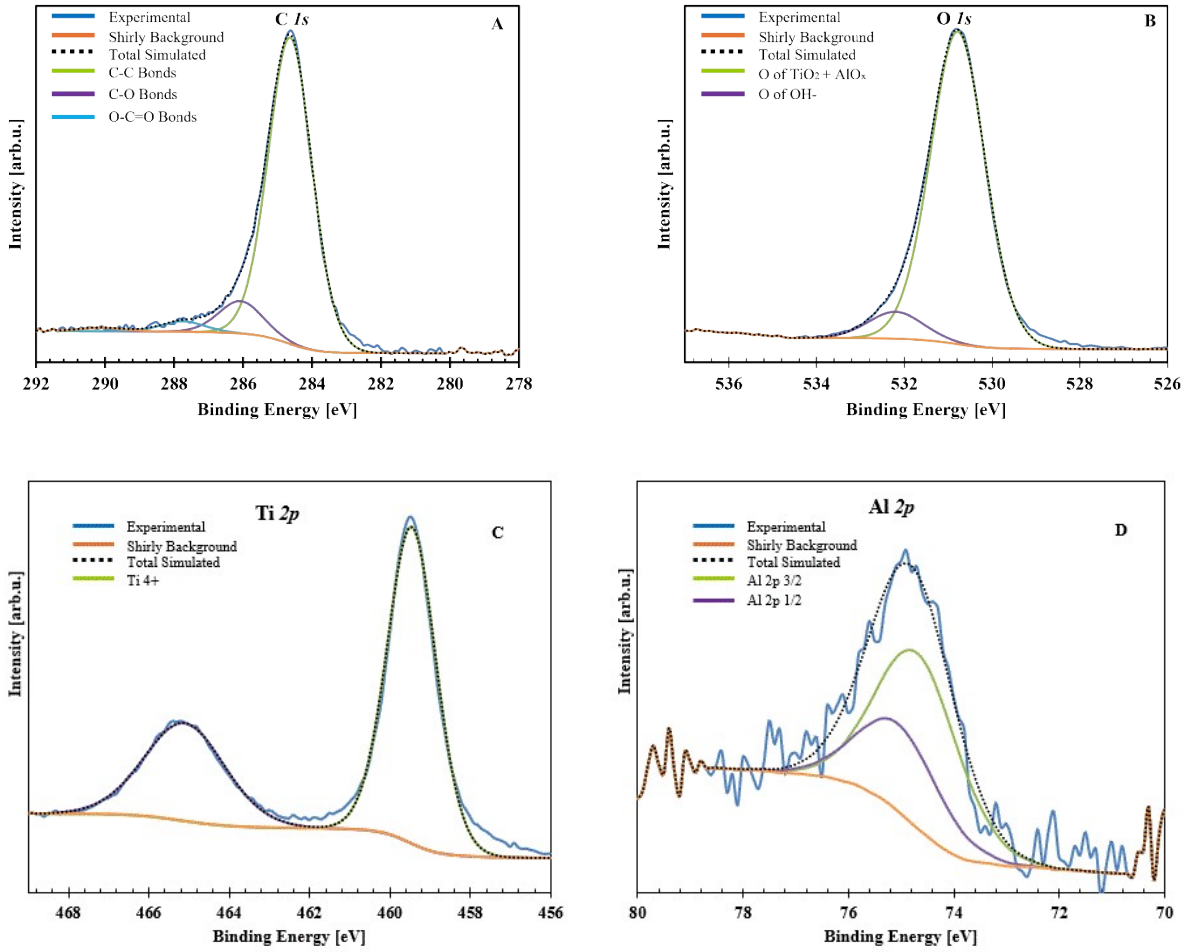


Figure S2: High-resolution XPS spectra of 1 ALD- $\text{AlO}_x$  deposited onto RF-sputtered  $\text{TiO}_2$ , fitted with a Shirley background, representing the respective elements of (A) C 1s, (B) O 1s, (C) Ti 2p, (D) Al 2p measured at a  $60^\circ$  emission angle.

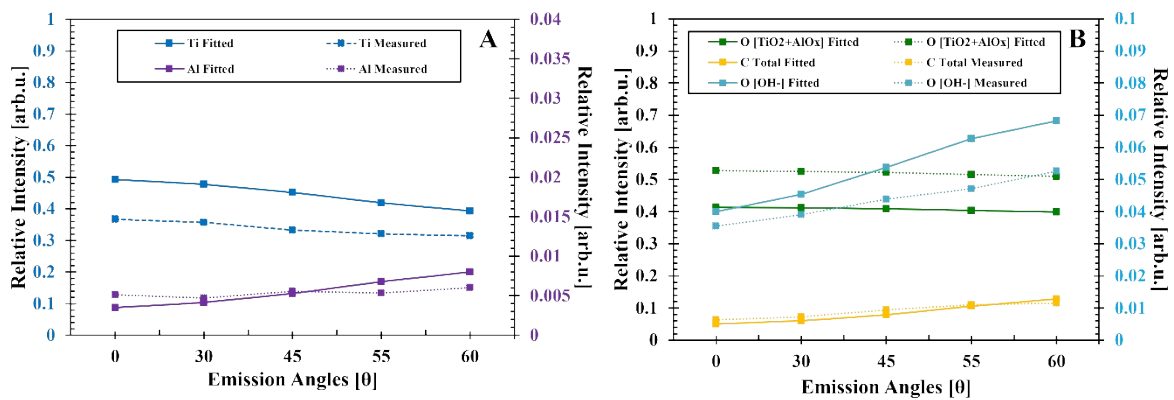


Figure S3: Variation in the ARXPS intensity of measured elements C, O, Ti, and Al versus the emission angles, solid lines connect the fitted intensity ratios, and the dashed lines connect the relative intensity of the measured data for the sample with deposition.

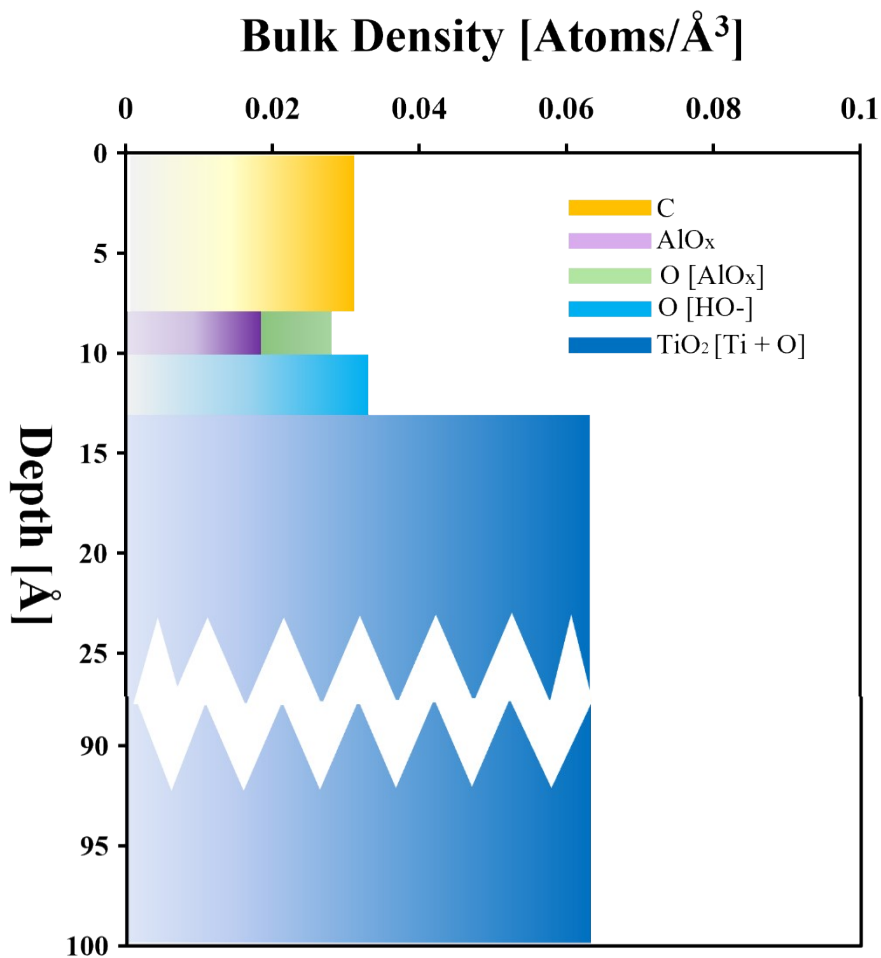


Figure S4: The concentration depth profile of the 1 ALD Cycle sample. The model presents the atomic densities of each emitting constituent element versus the depth in Angstrom ( $\text{\AA}$ ) within each respective layer.

### 5 ALD Cycle results (ARXPS)

The XP spectra of the four elements detected for high-resolution is presented in the main manuscript at a  $0^\circ$  emission angle. Figure S6. Shown the high-resolution of C 1s, O 1s, Ti 2p, and Al 2p at a  $60^\circ$  emission angle.

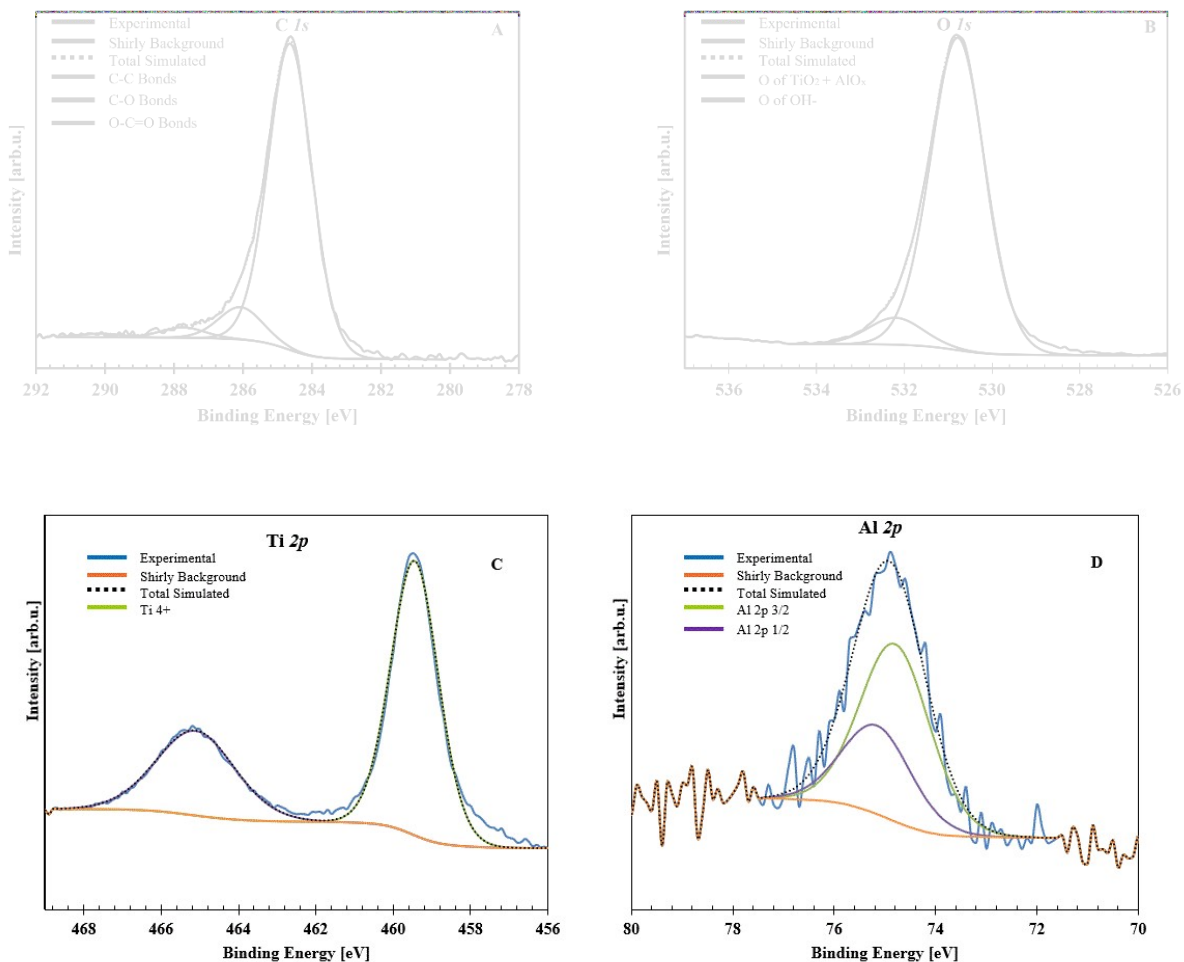


Figure S5: High-resolution XPS spectra of 5 ALD- $\text{AlO}_x$  deposited onto RF-sputtered  $\text{TiO}_2$ , fitted with a Shirley background, representing the respective elements of (A) C 1s, (B) O 1s, (C) Ti 2p, (D) Al 2p measured at a  $60^\circ$  emission angle.

### 10 ALD Cycle results (ARXPS)

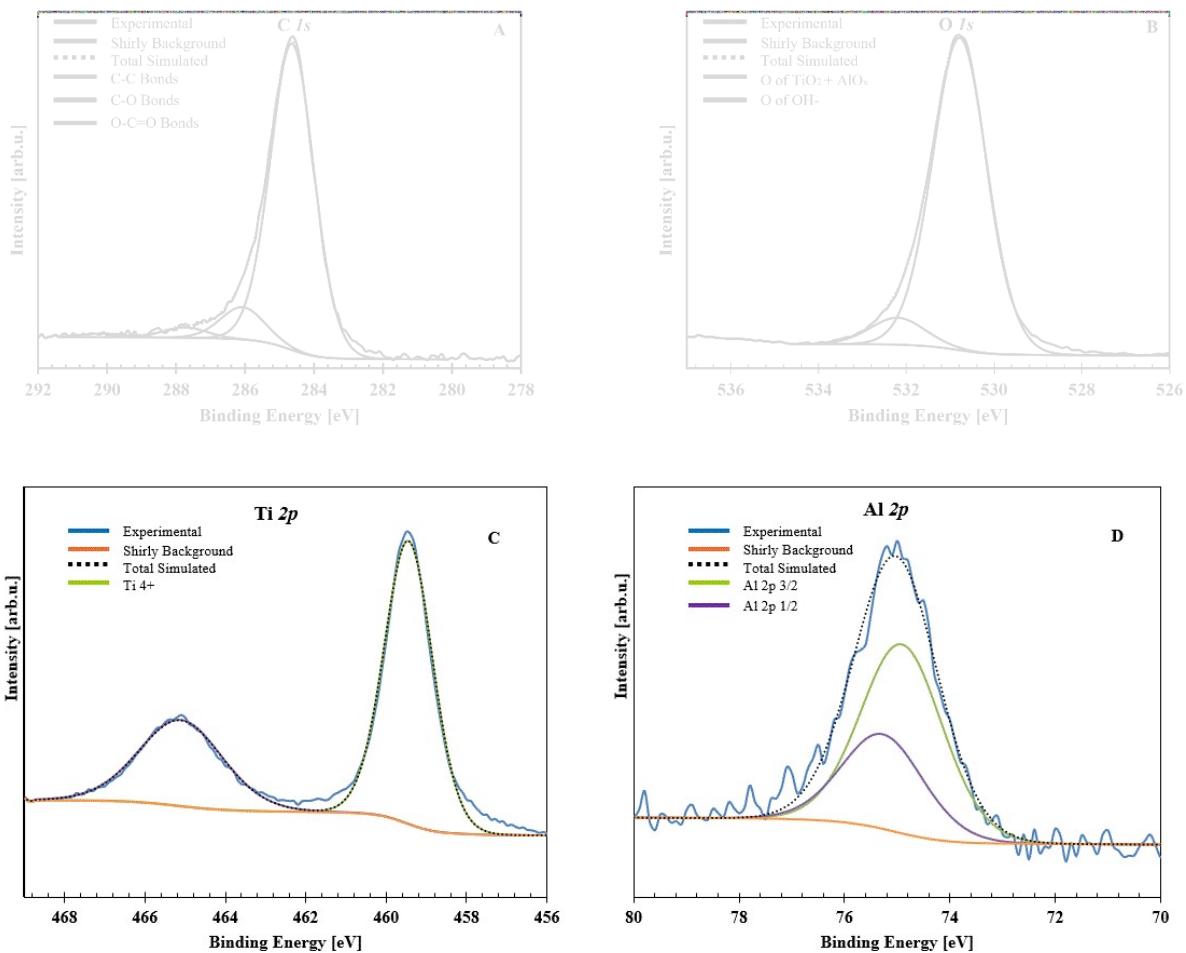


Figure S6: High-resolution XPS spectra of 10 ALD- $\text{AlO}_x$  deposited onto RF-sputtered  $\text{TiO}_2$ , fitted with a Shirley background, representing the respective elements of (A) C 1s, (B) O 1s, (C) Ti 2p, (D) Al 2p measured at a  $0^\circ$  emission angle.

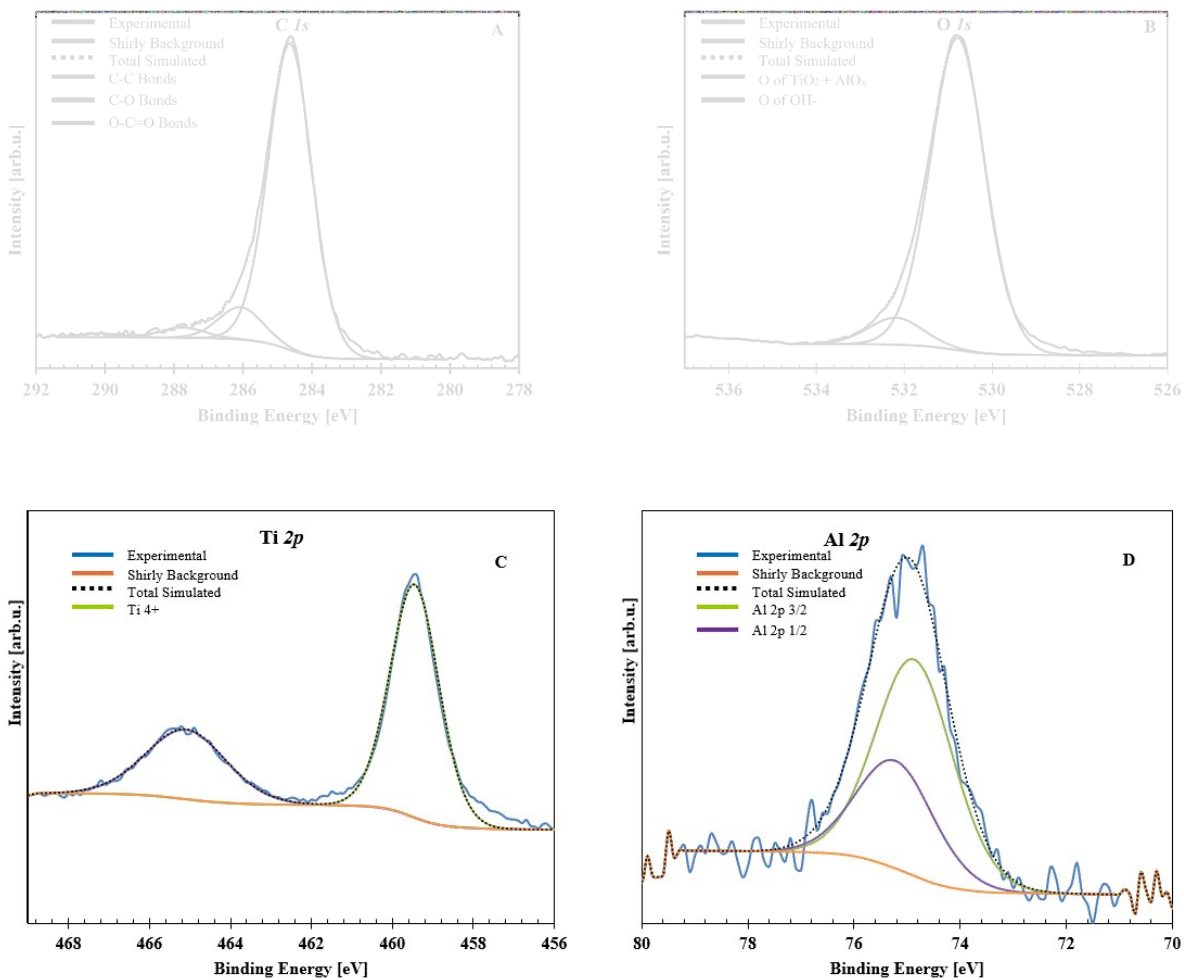


Figure S7: High-resolution XPS spectra of 10 ALD- $\text{AlO}_x$  deposited onto RF-sputtered  $\text{TiO}_2$ , fitted with a Shirley background, representing the respective elements of (A) C 1s, (B) O 1s, (C) Ti 2p, (D) Al 2p measured at a  $60^\circ$  emission angle.

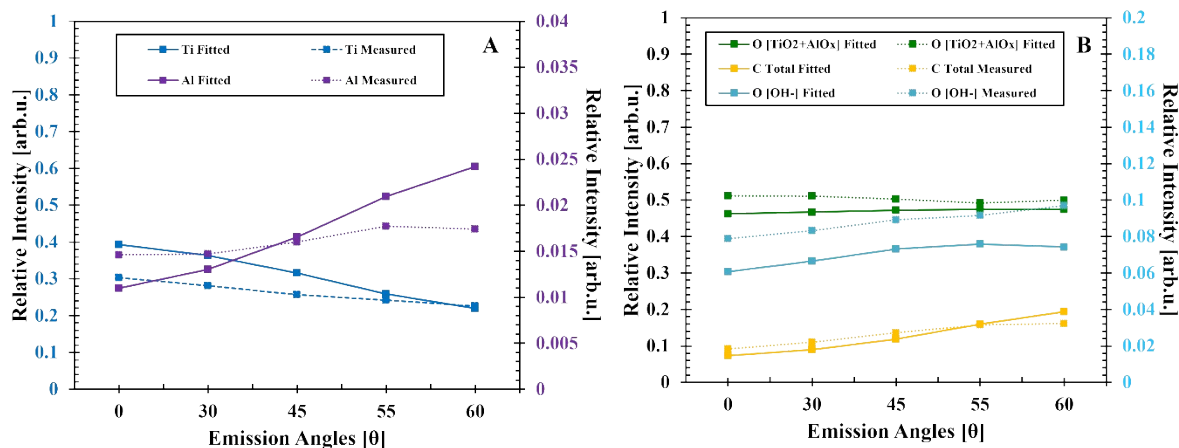


Figure S8: Variation in the ARXPS intensity of measured elements C, O, Ti, and Al versus the emission angles, solid lines connect the fitted intensity ratios, and the dashed lines connect the relative intensity of the measured data for the sample with deposition.

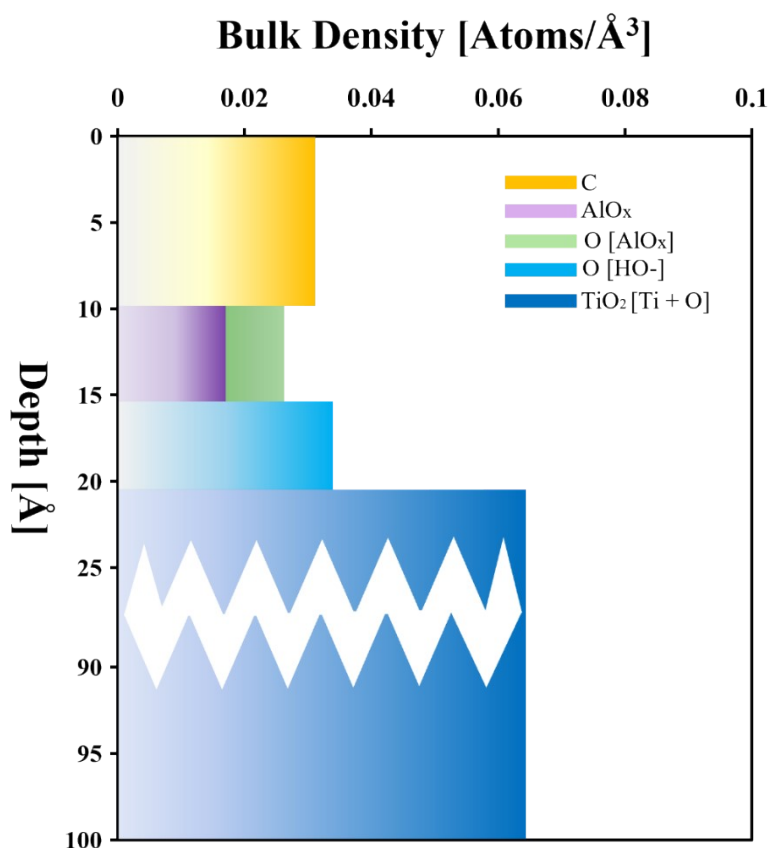


Figure S9: The concentration depth profile of the 10 ALD Cycles sample. The model presents the atomic densities of each emitting constituent element versus the depth in Angstrom (Å) within each respective layer.

## XPS Section

Table S4: Peak positions, peak intensity, and elemental composition of sample 1, 5, and 10ALD cycles of  $Au_{101}/TiO_2$  sample.

Sample \ Element		C			O		Ti	Al	Au
		Peak Position			Peak Position		Peak Position	Peak Position	Peak Position
		Peak 1	Peak 2	Peak 3	Peak 1	Peak 2	Peak 1	Peak 1	Peak 1
1 ALD $Au_{101}/TiO_2$	Before ALD	284.4	285.8	287.3	530.5	531.9	459.2	---	83.9
	After ALD	284.3	286.0	289.8	530.5	531.9	459.2	74.3	83.9
5 ALD $Au_{101}/TiO_2$	Before ALD	284.3	285.7	287.6	530.4	531.9	459.2	---	83.9
	After ALD	284.2	285.5	286.9	530.5	531.9	459.2	74.5	83.9
10 ALD $Au_{101}/TiO_2$	Before ALD	284.4	285.9	287.4	530.5	531.9	459.2	---	83.9
	After ALD	284.2	285.8	287.6	530.5	531.9	459.2	74.6	83.8
Sample \ Element		C			O		Ti	Al	Au
		Relative intensities			Elemental Composition		Elemental Composition	Elemental Composition	Elemental Composition
		Peak 1	Peak 2	Peak 3	Peak 1	Peak 2	Peak 1	Peak 1	Peak 1
1 ALD $Au_{101}/TiO_2$	Before ALD	10.0	1.6	0.6	58.9	3.6	23.4	---	2.0
	After ALD	9.5	1.7	0.3	56.0	4.0	19.9	6.9	1.7
5 ALD $Au_{101}/TiO_2$	Before ALD	7.2	1.2	0.3	60.9	4.0	24.1	---	2.3
	After ALD	7.7	1.6	0.5	52.7	8.4	16.8	10.5	1.9
10 ALD $Au_{101}/TiO_2$	Before ALD	7.9	0.9	0.4	60.9	3.6	24.2	---	2.1
	After ALD	9.8	2.1	0.6	45.3	13.6	11.9	15.5	1.4

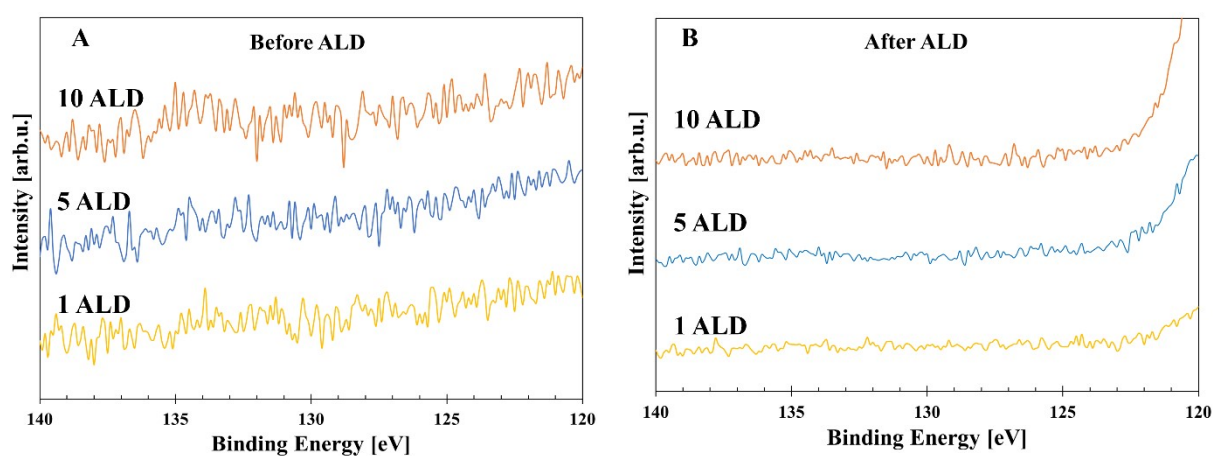


Figure S10: The high-resolution spectra of P 2p of the phosphine ligands (A) before ALD, and (B) after ALD of 1, 5, and 10 ALD cycles.

## ISS Section

For converting the sputtering dose into depth, it needs to be taken into account that during the sputtering process also material from the rest gas of the vacuum chamber is adsorbing onto the surface. Thus, the sum of sputtered material is the material sputtered from the sample as such plus the amount of gas adsorbing onto the surface of the sample during the sputtering process. The adsorption during sputtering has to be taken into account for a UHV pressure of a few  $10^{-10}$  mbar and depends on the composition of the UHV rest gas and the sticking coefficient of the gas molecules reaching the sample surface. The amount of material adsorbing onto the surface depends on the sticking coefficient of the surface and is significantly higher for an inorganic surface such as  $\text{AlO}_x$ , Au and  $\text{TiO}_2$  compared to a surface formed by hydrocarbons. The adsorption process is self-limiting in UHV because sticking of hydrocarbons and water is significantly reduced once the first layer has adsorbed from the rest gas. During sputtering this layer is removed making the surface more susceptible to fresh adsorption.

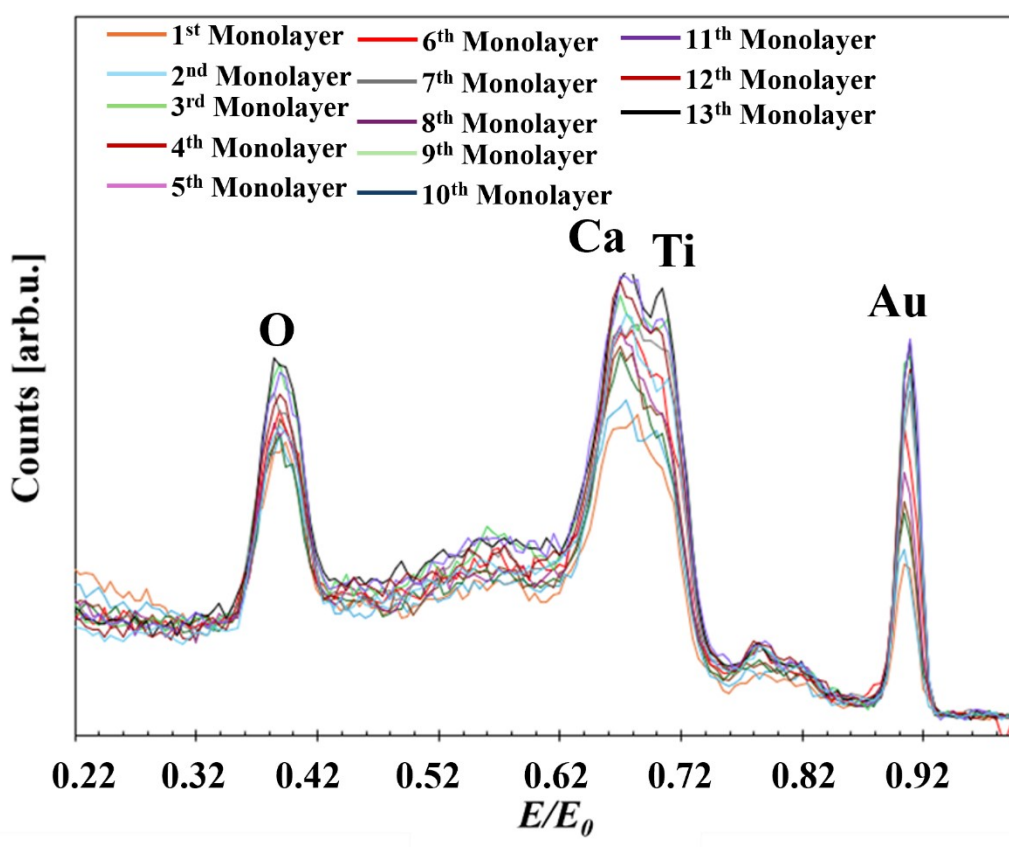


Figure S11: ISS survey spectra for  $\text{Au}_{101}/\text{TiO}_2$  sample. In the legend the number of sputtered monolayers is shown.

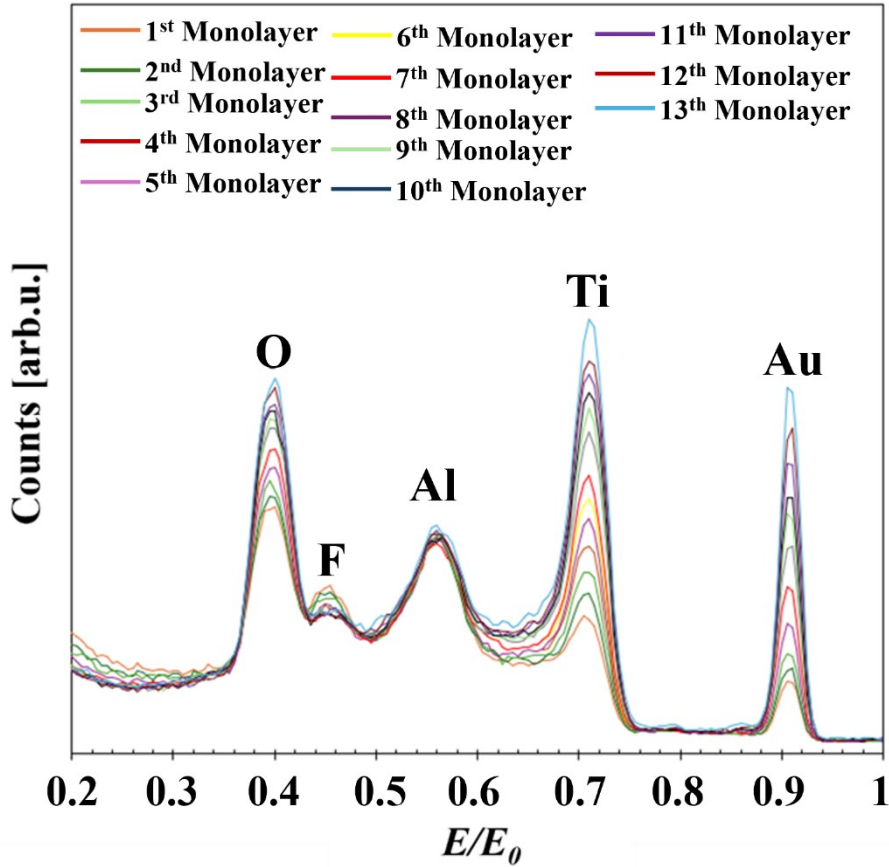


Figure S12: ISS survey spectra for 5 ALD AlO<sub>x</sub>/Au<sub>101</sub>/TiO<sub>2</sub> sample.

### ISS Monolayer Calculations

To convert the number of ISS scans (total number of scans 75) to sputtered monolayers we applied the following procedure,

The ion irradiation *irr* in C for a single scan is calculated as the product of the ion current per area times the time of the scan.

$$irr = t \cdot I = 34s \cdot 0.16 \cdot 10^{-9} A/mm^2 = 5.4 \cdot 10^{-6} C \dots eq.2$$

The total number of ions hitting the sample per scan is the irradiation divided by the elementary charge *e*.

$$Total\ No\ of\ Ions\ (hitting\ the\ sample\ per\ scan) = \frac{irr}{e} = \frac{5.4 \cdot 10^{-6} C}{1.60 \cdot 10^{-19} C} = 3.4 \times 10^{13} \dots eq.3$$

The ion dose is the number of ions per unit area that the ions hit. The area corresponding to the diameter of the ion beam is approximately 1 mm<sup>2</sup>.

$$\text{Total of Ions Dose} = \frac{\text{Total Number of Ions}}{\text{Area}} = \frac{3.4 \cdot 10^{13}}{1 \cdot 10^{-2} \text{ cm}^2} = 3.4 \cdot 10^{15} \text{ Ions/cm}^2 \dots \text{eq.4}$$

The sputter efficiency is a measure for how many sample atoms can be removed by a single projectile hitting the sample surface. In case of He a reasonable approximation is a sputter efficiency of 0.1 which means that approximately 10 He projectile remove one atom forming the sample.

The number of sputtered monolayers is calculated as

$$\text{Number of sputtered Monolayers} = \frac{\text{Total ion dose} \cdot \text{sputter efficiency}}{\text{Atoms per monolayer}} \dots \text{eq.5}$$

The number of atoms per monolayer is the number of atoms per unit cell divided by the area of the unit cell.

$$\text{Al}_2\text{O}_3: \# \text{ atoms/monolayer} = \frac{30}{(4.75 \cdot 10^{-8} \text{ cm})^2} = 1.3 \cdot 10^{16} \text{ atoms/cm}^2 \dots \text{eq.6}$$

The height of a  $\text{Al}_2\text{O}_3$  monolayer is 11.4 Ang assuming a cubic structure.

$$\text{TiO}_2: \# \text{ atoms/monolayer} = \frac{6}{(4.6 \cdot 10^{-8} \text{ cm})^2} = 2.8 \cdot 10^{15} \text{ atoms/cm}^2 \dots \text{eq.7}$$

The height of a  $\text{TiO}_2$  monolayer is 2.96 Å assuming a tetragonal rutile structure.

$$\text{Au: } \# \text{ atoms/monolayer} = \frac{4}{(4.08 \cdot 10^{-8} \text{ cm})^2} = 1.7 \cdot 10^{15} \text{ atoms/cm}^2 \dots \text{eq.8}$$

The height of a Au monolayer is 4.078 Å assuming a fccit structure.

The unit cell parameters are

$$\alpha\text{-Al}_2\text{O}_3: a = b = 4.75 \text{ Å}, c = \text{Å}$$

$$\text{Rutile TiO}_2: a = b = 4.59 \text{ Å}, c = 2.96 \text{ Å}$$

$$\text{Au: } a = b = c = 4.078 \text{ Å}$$

The number of sputtered monolayers is thus:

$$\text{Al}_2\text{O}_3: \frac{3.4 \cdot 10^{14}}{1.3 \cdot 10^{16}} = 2.6 \cdot 10^{-2} \text{ monolayers/scan}$$

$$\text{TiO}_2: \frac{3.4 \cdot 10^{14}}{2.8 \cdot 10^{15}} = 1.2 \cdot 10^{-1} \text{ monolayers/scan}$$

$$\text{Au: } \frac{3.4 \cdot 10^{14}}{1.7 \cdot 10^{15}} = 1.9 \cdot 10^{-1} \text{ monolayers/scan}$$

## NICISS Section

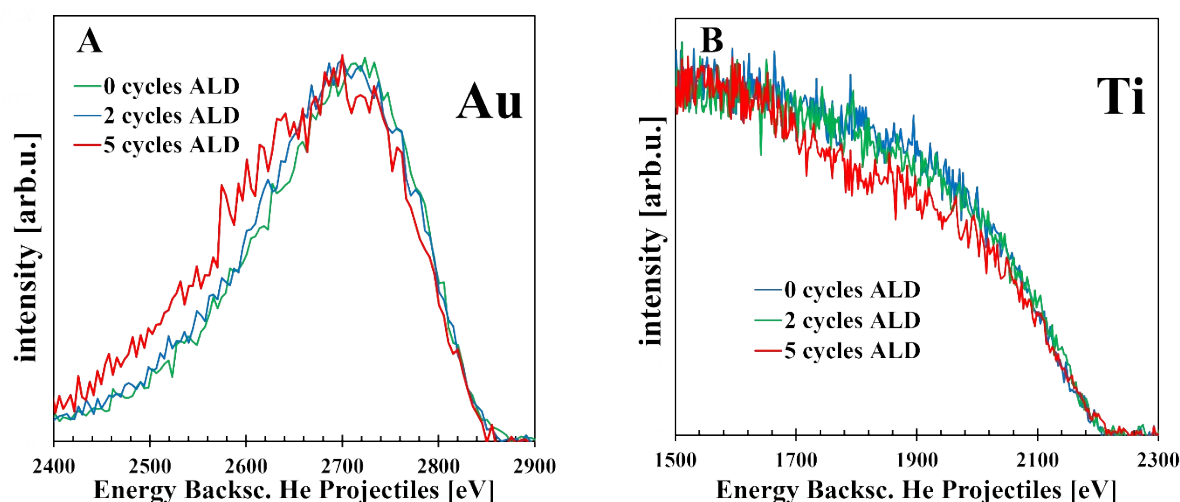


Figure S13: (A) NICIS spectra of gold and gold coated with 2 and 5 cycles of ALD- $\text{AlO}_x$  (B) NICIS spectra of titanium without ALD, with 2 and 5 cycles of ALD- $\text{AlO}_x$ .

### Determining the position of O of $\text{AlO}_x$ in XPS

A Si wafer  $1 \text{ cm}^2$  coated with 50 nm of Au was coated with  $\text{AlO}_x$ . Due to the presence of Au the O of  $\text{SiO}_2$  cannot be seen in the XP spectra. The O spectra before and after heating to  $250^\circ\text{C}$  for removing  $\text{OH}^-$  from the surface are shown. In A two O peaks and in B a single O peak are found. In A a peak at 531.0 eV corresponding to  $\text{AlO}_x$  and a peak at 532.2 eV corresponding to  $\text{OH}^-$  are found. In B a single peak at 531.5 eV corresponding to  $\text{AlO}_x$  is found.

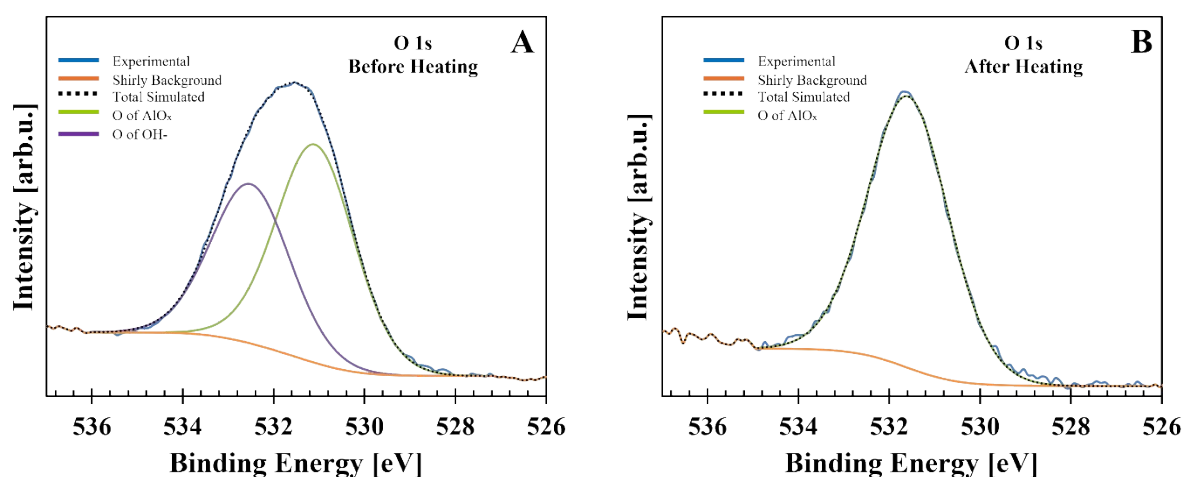


Figure S14: (A) O 1s spectrum for the O fitted with doublet peaks before heating the sample. (B) After heating the O 1s spectrum for the O fitted with a single peak.

### Iodine-iodide Exposure Experiment

The Au<sub>101</sub>/TiO<sub>2</sub> samples with 0, 1, 5, and 10 ALD cycles were exposed to an iodine-iodide solution to test how the Al<sub>2</sub>O<sub>3</sub> ALD overlayer can protect the covered Au<sub>101</sub> clusters against chemical reactions. Each sample wafer was placed in a sealed vial containing 2 mL of an iodine-iodide solution comprising KI (239.3 mg/mL) and I<sub>2</sub> (126.7 mg/mL) in MilliQ water.<sup>4</sup> The samples were exposed for 10 h then removed from the solution and immediately rinsed with MilliQ water and dried under flowing N<sub>2</sub>.

Two absorbance peaks in the UV-Vis spectra at 286 and 350 nm related to iodine species were observed for the iodide-iodine solution before exposure (Figure S15). Both peaks decreased significantly after the ALD Au<sub>101</sub>/TiO<sub>2</sub> samples were exposed to the solution. This indicates that the iodine species had reacted to form complexes such as [AuI<sub>2</sub>]<sup>-</sup> which do not absorb in these regions.<sup>4</sup>

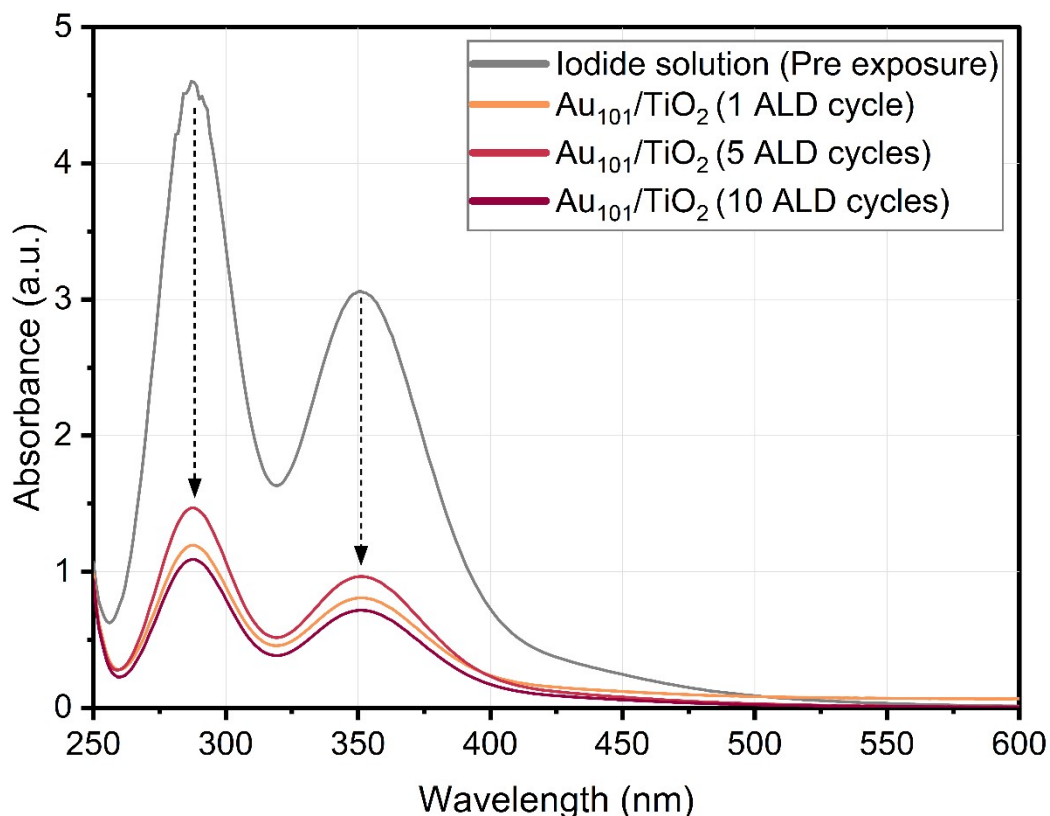


Figure S15: Absorption spectra of the iodine-iodide solution before and after exposure to Au<sub>101</sub>/TiO<sub>2</sub> with Al<sub>2</sub>O<sub>3</sub> overlayer samples for 10 h. Measurements performed with a Cary 3500 UV-Vis spectrophotometer.

Table S5 shows the change in relative intensity of the elements O, Ti, Al and Au representing the substrate, the Au clusters and the Al<sub>2</sub>O<sub>3</sub> overlayer. Figure S16 shows the XP spectra of Au

and Al of the 5 ALD on  $\text{Au}_{101}/\text{TiO}_2$  sample before and after iodine exposure. Before the iodine exposure, a clear Au 4f signal is observed. After iodine exposure, the Au signal intensity decreases significantly and becomes barely distinguishable from the background, indicating that the Au clusters are no longer detectable at the surface. The Al also decreases which could potentially be due to the removal of all Al species which are non-oxide species. While the Au clusters are mostly removed by this treatment, it remains questionable whether such treatment represents the chemical environment during the exposure to  $\text{H}_2\text{O}$  during photocatalysis.

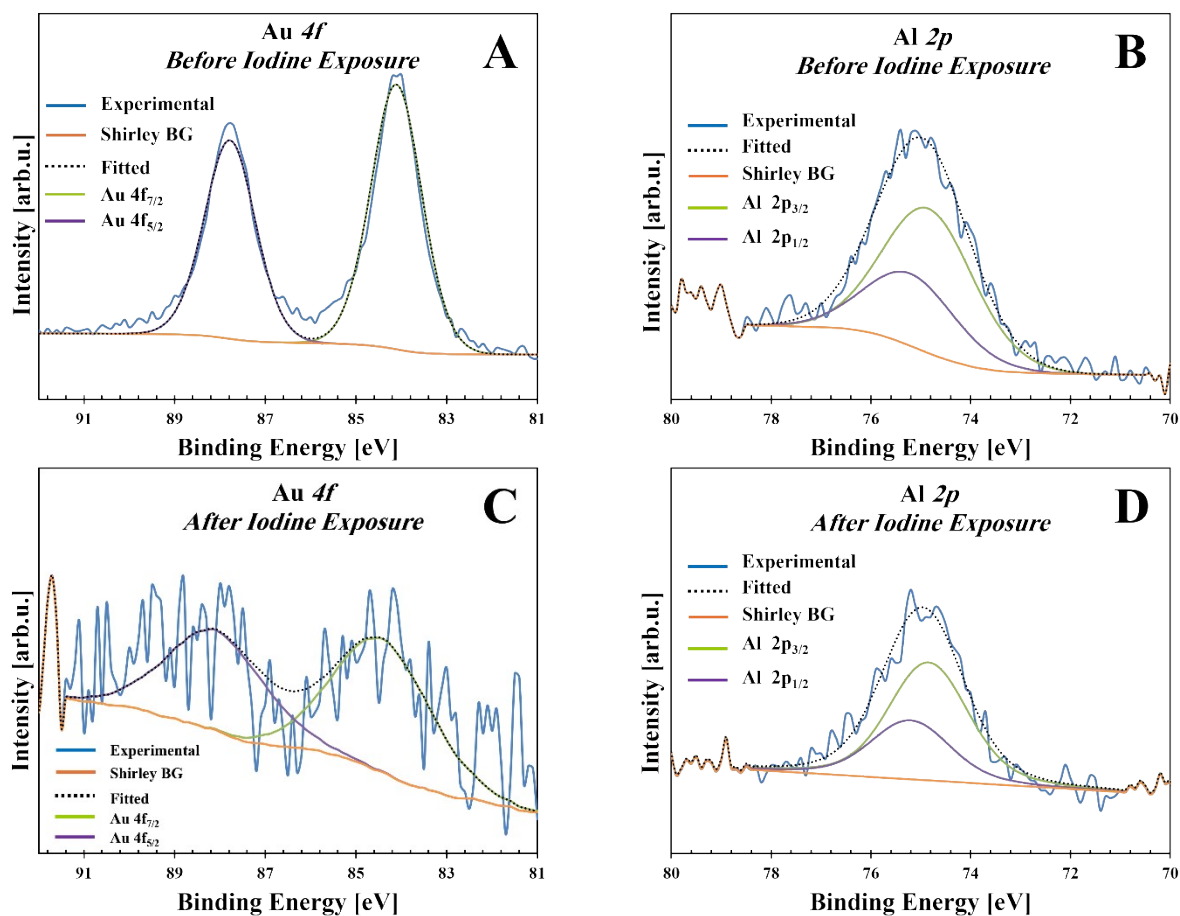


Figure S16: (A) Au 4f spectrum of the sample 5 ALD on  $\text{Au}_{101}/\text{TiO}_2$  before iodine exposure. (B) Al 2p spectrum before iodine exposure of the sample 5 ALD on  $\text{Au}_{101}/\text{TiO}_2$ . (C) Au 4f spectrum after iodine exposure, and (D) Al 2p spectrum after iodine exposure.

Table S5: Fraction of Al and Au remaining on the TiO<sub>2</sub> surface after applying the iodine procedure. For the calculation only the XPS peaks for the elements forming the substrate have been used, i.e. the O peak at 530.5 eV, the Ti, Al and Au peaks. The other O peaks and C are changing as well but only reflect the surface contamination due to the application of the iodine procedure and are thus not relevant for the analysis.

	XPS Intensity of O, Ti, Al and Au relative to the untreated sample [%]			
	O peak 1 (532.0 eV)	Ti (459.2 eV)	Al (74.7 eV)	Au (84.0 eV)
0 ALD Au <sub>101</sub> /TiO <sub>2</sub>	99	112	-	0
1 ALD Au <sub>101</sub> /TiO <sub>2</sub>	107	107	41	0
5 ALD Au <sub>101</sub> /TiO <sub>2</sub>	107	104	85	5
10 ALD Au <sub>101</sub> /TiO <sub>2</sub>	108	105	68	0

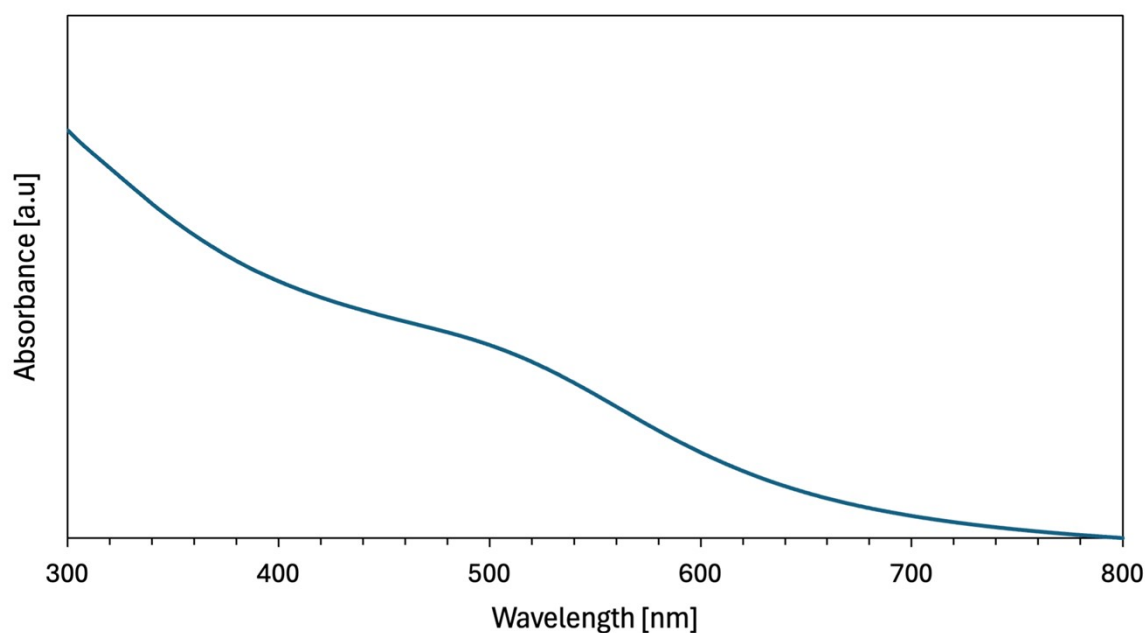


Figure S17: UV-vis absorption spectrum of Au<sub>101</sub> in dichloromethane.

## References

1. C. J. Powell, *Journal*, 2011.
2. J. J. Yeh and I. Lindau, *At. Data Nucl. Data Tables*, 1985, **32**, 1-155.
3. A. R. M. Alharbi, T. Roman, A. S. Alotabi, I. Köper and G. G. Andersson, *Langmuir*, 2024, **40**, 18925-18941.

4. M. Baghalha, *Hydrometallurgy*, 2012, **113-114**, 42-50.